THE JOURNAL OF PHYSICAL CHEMISTRY B

Article

pubs.acs.org/JPCB

Inter-Domain Interactions in Charged Lipid Monolayers

Benjamín Caruso,[†] Marcos Villarreal,[‡] Luis Reinaudi,[‡] and Natalia Wilke*,[†]

[†]Centro de Investigaciones en Química Biológica de Córdoba (CIQUIBIC), Dpto. de Química Biológica, and [‡]Instituto de Investigaciones en Físico-Química de Córdoba (INFIQC), Dpto. de Matemática y Física, Facultad de Ciencias Químicas, Universidad Nacional de Córdoba, Pabellón Argentina, Ciudad Universitaria, X5000HUA Córdoba, Argentina

Supporting Information

ABSTRACT: Phase coexistence is common in model biomembranes with the presence of domains formed by lipids in a dense phase state modulating lateral diffusion of species through hydrodynamic and electrostatic interactions. In this study, interdomain interactions in monolayers of charged surfactants were analyzed and compared with neutral systems. Interactions were investigated at different interdomain distances and by varying the ionic strength (I) of the subphase. At low percentages of condensed area (%Ac), i.e., high interdomain distances, domains were approximated as point charges or dipoles, and a comparison between the simulated and experimental results was made. At high %Ac, domains were arranged in a distorted hexagonal lattice, and the energy of a domain around its equilibrium position in the lattice was modeled using a harmonic potential and the spring constant determined. On subphases of high I, charged domains interacted in a manner similar to neutral domains with domain motion being precluded at high percentages of condensed area. At low I, a higher interdomain repulsion was observed along with a lower domain motion and, therefore, a higher apparent viscosity at comparable %Ac. Interestingly, this effect was observed at conditions where the Debye−Hückel length was still 2 orders lower than the interdomain distances.

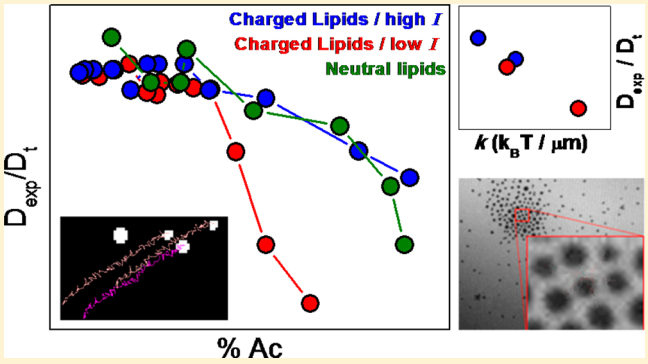

1. INTRODUCTION

Many model membranes show phase coexistence, characterized by ordered domains in a more fluid environment. It has been demonstrated that the presence of solid domains influences the diffusion of molecules residing either in the domains or in the continuum phase for systems formed by neutral, dipolar surfactants.[1−7] However, although charged lipid molecules (phosphatidylserine, phosphatidylglycerol, phosphoinositides, cardiolipin) are common in biological membranes, to the best of our knowledge, the influence of net charges on the apparent viscosity has not yet been explored.

The lateral diffusion of the components in membranes is a factor that determines, among others, the velocity of biochemical reaction−diffusion processes, and thus the function of cells.[8] The understanding of the diffusion process in membranes, involving complex two-dimensional fluid analysis, is an active research area that has still not been completely deciphered.[9] The presence of lipid domains in a dense phase state in a membrane affects the diffusion of the other species present in the membrane, since the domains act as rigid obstacles and furthermore provide an inhomogeneous scenario not only with respect to the rheological properties but also to the electrostatics. In fact, the electrostatic field generated by the domains can attract or repel the diffusing components, thereby influencing their lateral motion.[5,10]

When the domain density increases, interdomain interactions become important and their effect on the rheological properties of membranes becomes more noticeable.[10,11] The diffusion coefficient of domains and particles[4−7,10−12] as well as the radial distribution of domains in the plane of the membrane[11,12] have been used to estimate the strength of these interactions in membrane models such as GUVs and monolayers. However, to the best of our knowledge, the effect of charged lipids has not been considered.

Monomolecular layers at the air−water interface are frequently used as experimental models of natural membranes. In these systems, molecules are asymmetrically disposed at the interface, and form an array of charges (if present) and dipoles with a significant vertically oriented component, leading to electrostatic lateral repulsions between molecules which (together with line tension) contribute to determining the equilibrium shape and size of the domains.[13] Then, once formed, the domains will laterally interact according to their constituent dipoles and charges, as each phase presents a different dipole orientation and density, resulting in an excess dipole density being present in the domains.[13,14]

As mentioned above, charged lipid molecules are important components of biological membranes and it is recognized that the presence of net charges on the lipid molecules affects lateral interactions and consequently the phase diagrams in

Received: August 12, 2013
Revised: November 15, 2013
Published: December 17, 2013

bilayers.[15,16] Several studies have interpreted the effect of ionic strength on the phase diagrams of charged lipid containing bilayers to be related to a decrease in the Coulombic repulsion.[17] In the case of monolayers composed of charged lipids, Cëbers and Janmey proposed a model that accounts for the appearance of circular and irregular domains in mixed monolayer systems containing anionic lipids, and also demonstrated that the domain shape is further influenced by the ionic strength of the subphase.[18]

For the analysis of lateral interactions between domains in the presence of net charges on the amphiphiles, the ionic strength of the solution becomes an important variable, since the thickness of the electrical double layer induced by the charged membrane depends on the ionic concentration. With regard to this, Andelman et al.[19] described the interdomain interactions in monolayers of charged molecules with increasing values of ionic strength of the subphase, and identified the following two extreme regimes:

(a) For subphases with high ionic strengths, interdomain separation is large compared to the Debye−Hückel screening length (k^{-1}), and the electrostatic interactions between domains can be described by effective dipole moments, where the double layer is considered to be highly tied to the molecule.
(b) For subphases with low ionic strengths, k^{-1} increases, and when the interdomain distances are lower than k^{-1}, the interactions become Coulomb-like.

In other words, the ionic strength of the solution together with the distances between the domains both determine whether domains on a charged monolayer interact following a Coulomb or a dipolar regime.

The aim of the present study was to investigate possible differences in the interdomain interactions of micrometer-sized, charged domains and compare these with previously studied neutral domains.[6,7] Then, if the interactions between charged domains differed from those found in neutral domains, possible effects of the subphase ionic strength may emerge. Additionally, we wanted to assess how the presence of charged domains affects the global rheological properties of the membrane. With the purpose of trying to shed light on these issues, the interdomain interactions of charged domains were studied as a function of the percentages of area occupied by the domains using different approaches on subphases of different compositions.

2. EXPERIMENTAL SECTION

2.1. Materials. Dipalmitoyl phosphatidylglycerol (dpPG), distearoyl phosphatidylcholine (dsPC), dimiristoyl phosphatidylcholine (dmPC), and L-α-phosphatidylethanolamine-*N*-(lissamine rhodamine B sulfonyl) (ammonium salt) (egg-transphosphatidylated, chicken) were purchased from Avanti Polar Lipids (Alabaster, AL, USA). Tris(hydroxymethyl)-aminomethane (Tris) and NaCl were purchased from Sigma. The water used for the subphase was from a Milli-Q system (Millipore) with a resistivity of 18 MΩ cm and a surface tension of 72 mN/m.

2.2. Methods. *2.2.1. Preparation and Imaging of dpPG and dsPC/dmPC Monolayers.* The fluorescent probe (RhoeggPE) was incorporated into the lipid solution before being spread at a concentration of 1 mol % or less. Monolayers were formed in a Langmuir trough (Microtrough-XS, Kibron Finnland) on subphases containing 5 mM Tris buffer, pH 8.2 (low ionic strength), or this buffer plus 0.15 M NaCl (high ionic strength). The lipid mixture was dissolved in chloroform:methanol (2:1) to obtain a solution of 1 nmol/μL, which was spread onto the aqueous surface. Lateral pressure (determined with a Pt plate using the Wilhelmy method) and total film area were continuously recorded with a Kibron Microtrough-XS apparatus at rates between 1 and 2 Å^2 chain^{-1} min^{-1}, and the temperature was maintained at $T = 21 \pm 1$ °C. The error associated with the lateral pressure was about 1 mN/m, and for the mean molecular area (MMA), calculated as the trough area divided by the number of spread molecules, the error was 2 Å^2.

After spreading the lipid layer on an area 1.5 times the lift-off, the subphase level was reduced to a thickness of about 3 mm, in order to minimize convection. In addition, a glass mask with lateral slits extending through the film into the subphase was used to restrict the lateral monolayer flow under the field being observed.

The Langmuir balance was placed on the stage of an inverted microscope (Axiovert 200, Zeiss) equipped with a CCD IxonEM+ model DU-897 (Andor Technology) camera, a 20× long distance objective, a continuous solid state laser (TEM00, 532 nm up to 200 mW, Roithner Lasertech), and rhodamine emission filters. The fluorescent probe partitions preferentially on the LE phase and therefore the domains formed by lipid in a condensed phase appear darker in the images. To determine the amount of each phase, the original gray scale images were converted to binary (black/white) images using ImageJ. To carry this out, the slightly nonuniform illumination in the images (due to the intensity distribution across the laser beam profile) was removed using a band-pass filter and a particular gray scale level (threshold) was selected. Then, all pixels with intensities above this value were converted to "white", while pixels with intensities below this threshold level were converted to "black". The value of the threshold level was determined on the basis of an optimal resolution of the structures by performing a constant comparison with the original photo. Once a binary image had been obtained, the percentage of the total area occupied by the black regions was determined and named the condensed area percentage (%Ac). For the experiments where a region of crowded domains was generated by an electric field (see section 2.2.2), the %Ac was calculated within the region of recruited domains. The entire procedure for the calculation of %Ac along with an example and a discussion about the sources of errors and their usually found values are shown in section S2 of the Supporting Information.

2.2.2. Application of a Transitory Electric Field. In order to achieve a local crowding of domains, these were recruited by application of an electrical field.[20] Briefly, a metal wire was held at 200 μm above the subphase and a second electrode was placed in this subphase, with a potential difference being applied between the electrodes (Figure 2B, box f). The upper electrode was charged by applying potentials of up to 300 V with respect to the subphase electrode. It has been previously demonstrated that a positive potential leads to domain migration away from the zone of the interface under the electrode, whereas a negative potential generates the opposite effect as a consequence of the difference in the dipolar density of the phases in coexistence.[20,21] This migration of the domains generates a highly defined region of low (positive potential) or high (negative potential) domain density,[20,22] where the properties of the membrane under different crowding conditions of domains can then be analyzed.[7] This phenom-

enon has been observed in domains formed by both neutral and charged lipids,[21] since the effect is not governed by the characteristics of the polar headgroup, as demonstrated with fluorinated lipids.[23] Therefore, it was possible to achieve domain recruitment by the application of a negative potential difference to the upper electrode in all cases. When the desired domain density was obtained, the field was turned off and images were acquired. The areas of local high densities of domains thus obtained remained longer than the registration period of time of the experiment (more than 1 min, see the movie in the Supporting Information).

2.2.3. Domain Diffusion Coefficient Obtained from Their Brownian Motion. The determination of the diffusion coefficient of domains (D_{exp}) was performed as previously described.[7] Briefly, videos of the monolayer were recorded for 15 s at 10 frames/s. As explained in section 2.2.1, the original gray scale images were converted to binary (black/white) images. Then, the trajectories of the domains were followed through the 150 frames using the plugin "Mosaic" of ImageJ software.[24] Since convection may be reduced but not completely canceled, D_{exp} was calculated from the trajectories of two domains that suffered a similar convection drag (it was assumed that, at a close enough distance, $\lesssim$20 μm, the domains suffered the same drag). For an example of trajectories determined under convection drag, see section S3 of the Supporting Information. Considering the relative positions of domains at different time lapses between frames (δt), the mean square displacement (MSD) can be calculated using MSD = $|\vec{X}^{t+\delta t} - \vec{X}^{t}|^2$. This was then plotted as a function of δt for each pair of domains, and it was assumed that, if domains are of similar sizes, then the diffusion coefficients would be approximately the same. At these conditions, MSD = $8D\delta t$.[6,7] In order to evaluate possible artifacts due to an inadequate discount of convection drag or imprecision in the determination of the center of mass of each domain, a control for this technique was made by comparing the D_{exp} values with those predicted according to the theory of Hughes et al.[25] which is described in section 3.4. For the case of domains inside a region where they had been recruited by means of an electric field, domain motion was obtained from the tracking of domains placed at a distance from the edge of the recruited region of at least 10 times their radius. This was performed in order to avoid an "edge" effect, i.e, that domains tend to diffuse out to a less crowded region (which would led to a D_{exp} higher than the real value). In this manner, accurate D_{exp} values were obtained, since the determined values were similar to the calculated ones at a relatively low %Ac and since the interval of time related with the determination of D_{exp} was shorter than the characteristic relaxation time (usually, the recruited regions relax within several minutes).

2.2.4. Radial Distribution of Domains in the Plane of the Monolayer. The radial distribution function of the domains in the plane of the monolayer ($g(r)$) was calculated at different lateral pressures. To carry this out, three histograms of r (r = distance between domain centers) were constructed at each condition using the data from 50 consecutive frames obtained for homogeneous monolayers (without application of an electric field) and with the reported $g(r)$ being the average of these three histograms. Binning was tested from 1.1 to 2.2 μm, and a value of 1.6 or 1.7 μm was selected as an intermediate value, which was low enough in order to achieve a defined curve but high enough to reduce error.

2.2.5. Radial Distribution Functions from Molecular Dynamics Simulations. The $g(r)$ functions were calculated from molecular dynamics simulations (MD) in two dimensions, with the number of particles, the total area of the system, and the temperature being kept constant. In the simulations, each particle represented an idealized lipid domain with a mass determined from the average number of lipids in the domain, which was inferred from the monolayer micrographs and compression isotherms (MMA). The simulated systems consisted of 50 particles under periodic boundary conditions, using the minimum image convention. The area was adjusted to match the experimental surface domain density, and the temperature was controlled using a Langevin thermostat. In the MD simulations, the particles interacted with a pair potential of the form Num/r^{-n}, where Num and n are constants and r is the distance between particles. The values of n selected were 1 or 3, which correspond to a Coulomb or dipolar interaction, respectively. The values of Num were systematically varied in order to find the best match between the experimental and simulated $g(r)$, using the root-mean-square deviation (RMS) between curves as a measure of similarity. Thus, the reported Num is the value for which the calculated $g(r)$ has the minimum RMS (RMS_{min}) with respect to the experiment. The errors in the Num values were estimated from the possible values of Num that resulted in RMS being within the 10% of the RMS_{min} (see section S5 in the Supporting Information).

All the simulations were performed with an in-house program. A 3D version of the program using the Lennard-Jones potential was checked against the results from the well-known GROMACS package, in order to ensure our program was functioning correctly. To check for system size dependency, systems with 100 and 200 particles were simulated, with no changes being found in the calculated $g(r)$ functions.

2.2.6. Quantification of Interactions between Domains at High %Ac Regimes. These calculations were performed with recruited domains following the procedure described in section 2.2.2. From videos of the recruited regions (150 frames, 15 s), the positions of seven domains of similar sizes forming a hexagonal lattice (with one central domain and six close neighbors) were tracked. Then, using these data, the center of mass of the six domains surrounding the central domain was calculated. The position of the central domain in relation to the center of mass was obtained for each frame, and the frequency distribution of these positions was adjusted using a fitting equation as explained in section 3.5. In this analysis, hexagonal arrays in the recruited region that were surrounded by at least two anneals of domains of similar density were chosen and the distribution of the position of the central domain in the array was assumed as in a local equilibrium. %Ac was calculated in the whole recruited region (for an example, see Figure 7A). This procedure did not lead to additional error in the determination of %Ac (see more detail in section S2 of the Supporting Information).

3. RESULTS AND DISCUSSION

3.1. Compression Isotherms of the dpPG Monolayers.

Dipalmitoyl phosphatidylglycerol (dpPG) is an anionic lipid whose pK_a's on membranes have been reported to be between 1 and 2.9 (see Egorova[26] and references therein). The ionic state of a molecule organized at an interface depends on the surface pH, which was calculated according to the Gouy–Chapman model, for different salt concentrations as reported in Vega Mercado et al.[27] From these results (shown in section S4

dx.doi.org/10.1021/jp408053a | J. Phys. Chem. B 2014, 118, 519–529

of the Supporting Information), a subphase pH of 8.2 was chosen in order to ensure a completely dissociated polar headgroup. This pH was achieved with a Tris buffer at a 5 mM concentration, which implied that the condition of lower salt concentration led to an ionic strength (I) of 5 mM (the basic species is neutral) and a corresponding Debye−Hückel length (κ^{-1}) of 4.3 nm. Lower buffer concentrations did not prevent acidification of the subphase due to CO_2 dissolution. The high ionic strength solution corresponded to the same buffer plus 0.15 M NaCl (I = 0.305 M and κ^{-1} = 0.55 nm).

The compression isotherms of the dpPG monolayers (Figure 1) exhibited a typical liquid-expanded to liquid-condensed

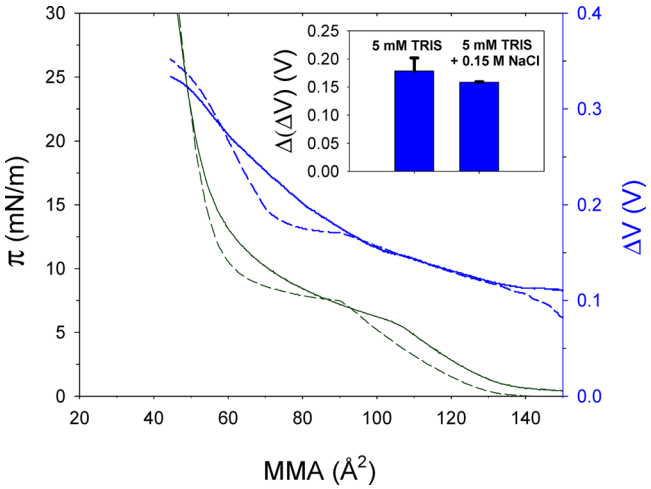

Figure 1. Representative compression isotherms showing π (green) and ΔV (blue) vs MMA of dpPG monolayers on Tris buffer 5 mM (pH 8.2) in the absence (solid lines) or presence (discontinuous lines) of 0.15 M NaCl. Inset: ΔV differences, $\Delta(\Delta V)$, between liquid-expanded and liquid-condensed phases. ΔV values were taken at the beginning and at the end of the phase transition (n = 3). The temperature was 21 ± 1 °C.

phase transition beginning at surface pressures of 6.5 and 7.5 ± 1 mN/m for low and high ionic strengths, respectively. When observed under the microscope, the domains appeared at the same surface pressures as the onset of the phase transition in each monolayer. The difference in the onset of the phase transition as well as of the subsequent slope were statistically significant; i.e., the phase transition in the presence of salt started at higher pressures and also occurred at a smaller range of pressures. Moreover, once the domains appeared, they grew faster, and the change in the percentage of condensed area with pressure during the phase transition was higher for monolayers in the presence of salt (compare the example values in Figure 2A). These changes cannot be attributed to a difference in the dissociation degree of the polar headgroup as in Grigoriev et al.,[28] since, as already mentioned, conditions were selected in order to ensure a 100% charged monolayer. Our results are in good agreement with the observation of Ruckenstein et al.[29] who explained the absence of a zero slope during the phase transition by considering electrostatic repulsion between domains and also with the experimental observations of Aroti et al.[30] with monolayers of dipalmitoyl phophatiyilcholine, who suggested that anions bind to the looser liquid-expanded phase and do not penetrate into the domains of the liquid-condensed phase.

The surface potential (ΔV) was similar for both systems, but in the presence of NaCl, a plateau similar to that in the surface pressure isotherm was observed. This effect (which is related to rearrangements of the ions at the interface and/or the dipole of water and of the surfactant as the monolayer is compressed) may also be present in the absence of NaCl but in a less cooperative fashion, as happened with the surface pressure isotherm. The surface potential difference between phases, $\Delta(\Delta V)$, was calculated as the difference between the liquid-condensed (ΔV_{LC}) and the liquid-expanded (ΔV_{LE}) phases, with ΔV_{LE} being taken at the onset of phase transition and ΔV_{LC} at the point where the whole monolayer was in the condensed phase (as observed using the microscope, which coincided with the acquisition of a constant slope in the compression isotherm). This yield averaged values (from three independent experiments) of $\Delta(\Delta V)$ = 0.18 ± 0.02 and 0.160 ± 0.001 V in the absence and presence of NaCl, respectively, with no significant statistical differences being found (inset in Figure 1).

The distributions of domain radius (calculated from the domain size assuming circular domains) are shown in Figure 2A for two representative monolayers with or without 0.15 M NaCl in the 5 mM Tris subphase. Figure 2Ba−c shows an example of a monolayer in the absence of NaCl at progressive degrees of compression evidencing that, once a domain appeared, they grew upon compression. Domain interactions were evaluated as a function of the percentage of monolayer surface covered by domains (named %Ac), which is a parameter that depends on both domain size and interdomain distance. For each surface pressure, %Ac was calculated as explained in section 2.2.1, and the obtained values are detailed in Figure 2A. In the absence of NaCl, the domain sizes presented a narrow distribution within the analyzed surface pressure range (6.4−8.4 mN/m), which corresponded to a %Ac up to 10.8%. In contrast, when NaCl was present in the subphase, the distribution of domain sizes was narrow up to % Ac of approximately 5% (corresponding to 10 mN/m).

For both ionic strengths, further compression of the monolayer induced domain growth rather than the appearance of new domains, with more polydisperse domain size distribution being observed for monolayers on subphases with NaCl than in the absence of salt, as previously reported for neutral monolayers.[30]

3.2. Radial Distribution of the Domains in the Plane of the Monolayer. In order to describe the lateral distribution of domains, the radial distribution function ($g(r)$) at different %Ac was calculated for the dpPG monolayers on subphases with or without NaCl, and also for monolayers of dmPC/dsPC (x_{dsPC} between 0.3 and 0.5 and at a fixed lateral pressure of 10 mN/m) on the same subphases (Figure 3). These latter monolayers were included for comparison, as an example of a system with neutral (dipolar) domains, whose rheological properties as a function of %Ac were previously studied by our group in the absence of Tris[6] and at slightly higher temperatures, 23 °C.[6] The compression isotherms of both phospholipids are shown on the different subphases in Figure S1 (Supporting Information). %Ac was increased by increasing the surface pressure in the case of dpPG monolayers and increasing the proportion of dsPC at a fixed surface pressure for monolayers composed of the PC mixture.

In all cases, the $g(r)$ function resembled that of a gas (no structure) for low %Ac values, and a peak appeared (corresponding to the nearest neighbor distance in an ordered

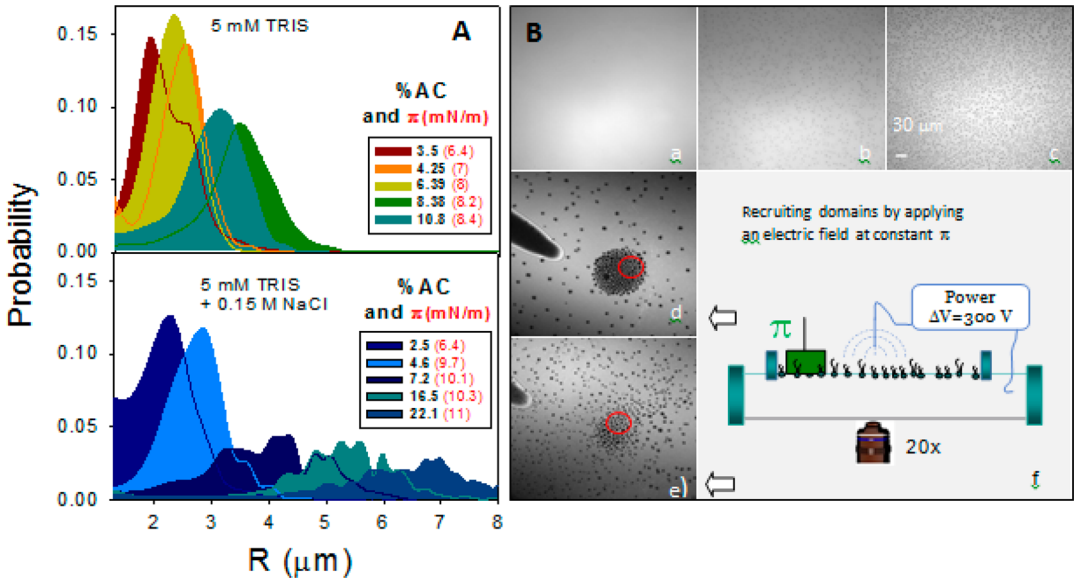

Figure 2. (A) Domain size distribution of monolayers at different degrees of compression, expressed as %AC (or π) on low (upper plot) and high (lower plot) ionic strength 5 mM Tris subphase. (B) Fluorescence images of dpPG monolayers on subphases with Tris buffer (without NaCl) at π values lower than the phase transition (3 mN m^{-1}) (a) and for π exhibiting disordered (6.4 mN m^{-1}) (b) or ordered (8 mN m^{-1}) (c) domain spatial distribution. The fluorescent probe Rho-eggPE partitions preferentially in the liquid-expanded phase. After application of a non-homogeneous electric field, domains were recruited in order to obtain higher domain densities at a desired π (d, e, examples at 8.4 mN m^{-1} in the abscence and 8 mN m^{-1} in the presence of 0.15 M NaCl, respectively). The percentage of condensed area for these experiments was calculated in a circular region centered on the particular domains under study. In this example, the region is marked in red (see details in section S2, Supporting Information). (f) Scheme illustrating the experimental setup used for applying a transitory electric field on the monolayer.

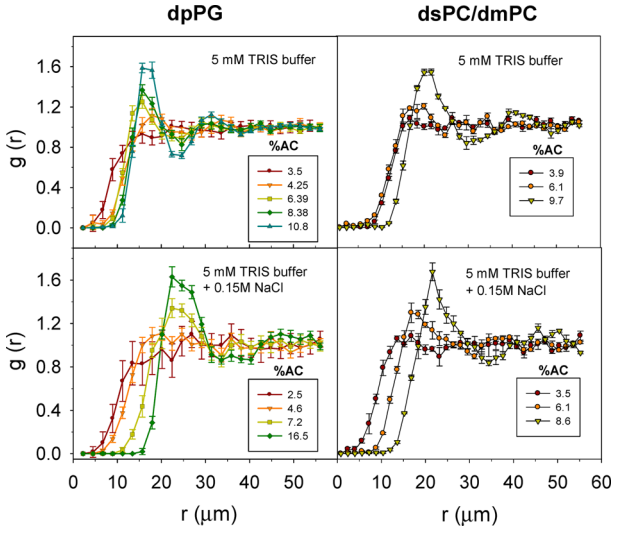

Figure 3. Radial distribution functions, $g(r)$, for the four systems analyzed: monolayers of the anionic dpPG (left) or the neutral dsPC/dmpC mixture (right) on a subphase of 5 mM Tris pH 8.2 with (bottom) or without (top) 0.15 M NaCl. Each condition was analyzed at variable %Ac (as indicated in the legends). Each point represents the average ± standard deviation, as explained in section 2.2.4.

array) as the percentage of condensed area increased. As an example, see the images in Figure 2Bb and c for a disordered with very small domains and an ordered monolayer, respectively. For monolayers of dpPG on subphases without NaCl, this peak appeared at %Ac between 3.5 and 4.25%, at a distance of r = 18 μm.

In the presence of 0.15 M NaCl in the subphase, the dpPG monolayers exhibited the peak corresponding to the nearest neighbor at higher values of %Ac. According to this peak, the nearest neighbors in these systems were found at r = 22 μm, a similar distance to monolayers composed of neutral lipids (dmPC/dsPC), where the first peak appeared at r = 21 μm. These neutral monolayers were not affected by the presence of Tris, as they were comparable to those reported on NaCl subphases.[6] Neutral monolayers presented similar $g(r)$ curves with a defined structure (emergence of a peak) at a %Ac value of about 6% on 0.15 M NaCl and on 5 mM Tris with or without 0.15 M NaCl at temperatures between 21 and 23 °C.

At higher %Ac, a second peak appeared around 30 μm on dpPG without NaCl. On neutral lipid monolayers and dpPG with 0.15 M NaCl, this peak was less evident and broader and appeared at higher r values.

All of these above observations suggest a similar behavior between monolayers of dpPG on 0.15 M NaCl and neutral monolayers, whereas dpPG monolayers in the absence of NaCl presented a different trend. The interdomain repulsion appeared to be lower for the neutral monolayers and the monolayers of dpPG on NaCl, compared with dpPG monolayers on a subphase without NaCl, since an ordered array of domains was observed at higher %Ac. In order to obtain quantitative information about interdomain interactions within the $g(r)$ function, simulations were made which utilized Coulomb and dipolar electrostatic interactions, as detailed in the following section.

3.3. Comparison of Experimental and Simulated Radial Distribution Functions. Interdomain Interactions at Conditions of Low %Ac. In order to gain insight into the radial dependence and the strength of the interdomain interactions in each system, two extreme regimes were evaluated—Coulomb and dipolar interactions—assuming the following interaction energies:

dx.doi.org/10.1021/jp408053a | J. Phys. Chem. B 2014, 118, 519−529

$$U = \frac{q^2}{4\pi\varepsilon_0\varepsilon} \times \frac{1}{r} \quad (1)$$

$$U = \frac{\mu^2}{4\pi\varepsilon_0\varepsilon} \times \frac{1}{r^3} \quad (2)$$

where q and μ are the charge and dipole excess, respectively, in the liquid-condensed phase relative to the liquid-expanded phase. ε_0 is the vacuum permittivity (8.854×10^{-12} F m^{-1}) and ε is the relative permittivity of the membrane, which was approximated to a value of 2.

For the simulation of the radial distribution functions, $g(r)$, a nVT system was allowed to equilibrate. Each simulation consisted of a particular domain mass and density, which were equal to the average experimental values determined at each %Ac; for the simulations, polydispersity was not considered. As explained in section 2.2.5, different domain spatial patterns (and consequently, different $g(r)$) were obtained according to the value of Num chosen in the following expression, which determines the energy of interaction of the simulated domains:

$$U = \frac{\text{Num}}{r^{-n}} \quad (3)$$

Then, considering $n = 1$ or $n = 3$ for each model, the procedure used was to systematically vary the value of Num in order to find the best fit to the experimental curves, as measured by the root-mean-square deviation (RMS) between experimental and simulated curves. A representative example of the variation of RMS as a function of Num and the procedure used to estimate the error in Num are shown in the Supporting Information (section S5).

The above equations consider the domains to be point charges (eq 1) or point dipoles (eq 2), which, however, is only an approximation, since domains are formed by a discrete number of charges and/or dipoles. Consequently, considering domains to be point dipoles or charges is not a good approximation at low interdomain distances, where the discrete nature of the lipid−lipid interaction should be taken into account (high %Ac values). Related to this, it has been demonstrated that, as two domains formed by neutral molecules approximate to each other, the dependence of the interaction with the separation departs from that described by eq 2.[12,31] Hence, our analysis was restricted to low %Ac, as detailed below.

In Figure 4, the experimental and simulated curves (representing the best fit) are plotted for representative curves at each condition, with other experiments being depicted in the Supporting Information (section S6).

The minimal values for RMS (RMS_{min}) obtained by varying Num for both exponent values (i.e, r^{-1} and r^{-3}) are plotted in Figure 5 as a function of the percentage of the condensed area. As expected, the domain distribution in neutral monolayers (in the absence or presence of NaCl in the subphase) was best fitted with dipole−dipole interaction energy at low %Ac (<9%). Interestingly, this trend reverted from r^{-3} to r^{-1} at %Ac values between 7 and 8%, and clearly, this switch cannot be explained as a change from a dipolar to a Coulomb regime. In these neutral systems, the rise in %Ac was implemented by a change in the lipid composition which led to more crowded domains of similar sizes.[6] Therefore, as %Ac increased, the domains were forced to be closer to each other. According to Wurlitzer et al.,[14] dipolar interaction forces can exhibit different radial dependencies according to the domain separation (S) and their radius (R) especially at experimentally relevant intervals ($0.1 < S/R < 10$), where the strength of the interaction should vary between the asymptotic $(S/R)^{-1/2}$ and $(2 + S/R)^{-4}$ dependencies, at low and high S/R, respectively. A similar behavior has been suggested for the electric field generated by a dipolar domain, with a transition from a regime of a domain as a single dipole to a domain formed by a semi-infinite region of

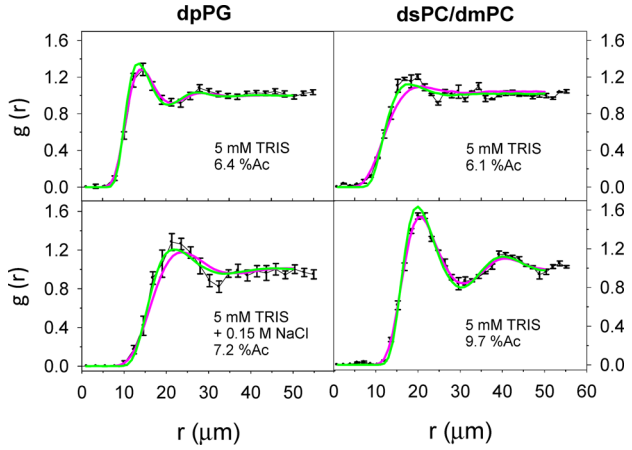

Figure 4. Radial distribution functions, $g(r)$, obtained experimentally and from molecular dynamics simulations. Left: anionic dpPG monolayers on 5 mM Tris pH 8.2 with (bottom) or without (top) 0.15 M NaCl at the indicated %Ac. Right: neutral dsPC/dmPC monolayers on 5 mM Tris subphases at %Ac where either the r^{-3} model led to a better fit (top) or where the r^{-1} model led to a better fit (bottom) to the experimental data. Black symbols and line, experimental; magenta line, Coulomb interaction model; green line, dipolar interaction model. Each experimental point represents the average ± standard deviation, as explained in section 2.2.4.

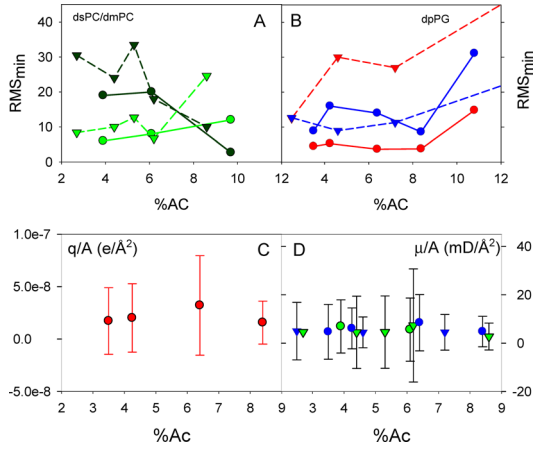

Figure 5. Minimal values of RMS obtained after systematic variation of Num values in eq 3 for neutral (A) and charged (B) monolayers in the absence (circles/solid lines) and presence of NaCl (triangles/dashed lines) in the subphase and using an r^{-1} (dark green in A and red in B) and r^{-3} (light green in A and blue in B) radial dependence for the domain−domain interactions. (C and D) Excess surface charge (q/A) and dipole density (μ/A) between phases, calculated from the Num values that yielded minimal RMS using eqs 1 and 2, respectively. (C) q/A values for dpPG monolayers in the absence of NaCl. (D) μ/A values for neutral monolayers in the absence (light green circles) and in the presence of NaCl (light green triangles) and dpPG in the absence (blue circles) and in the presence (blue triangles) of NaCl.

dx.doi.org/10.1021/jp408053a | J. Phys. Chem. B 2014, 118, 519−529

dipoles.[12] Rückerl et al. proposed (based on Monte Carlo simulations) that the distance dependence of the electric field can present two distinguishable regimes depending on the domain size: for small domain radius, the electric field exhibits an r^{-3} dependence (single dipole regime), whereas for bigger domains it exhibits an r^{-1} dependence (semi-infinite field of dipoles).

Taking the above observations into account, the change noted for the best fit to the experiments from eq 2 to eq 1 as %Ac increased may have been a consequence of the fact that the domains got closer to each other as %Ac increased. Therefore, as the point dipole was no longer a good approximation, then the interaction of all pairs of dipoles in each domain should be computed. Consequently, all the discussions of interdomain interaction from the $g(r)$ function will be restricted to %Ac $\leq$ 9%.

For dpPG monolayers, the model that better fitted the experimental curves depended on the presence of NaCl in the subphase (Figure 5B). In the case of dpPG monolayers without NaCl in the subphase, the Coulomb interaction model presented lower values of RMS_{min} in the analyzed %Ac. However, it is worth pointing out that considering dipolar interactions also led to a good modeling of the experimental data (Figure 5B and section S6.1, Supporting Information) and, thus, using this approach it is not possible to accurately distinguish between both interaction models. It is possible that an intermediate regime (neither dipoles nor charges) is ruling at this ionic strength condition (see below). In contrast, in the presence of NaCl, the dipolar interaction led to a clearly better fit to the experimental data. For both dpPG systems, the values of RMS_{min} remained relatively constant up to a value of %Ac of about 10% (when the domain sizes became more polydisperse, see Figure 2A), after which the RMS_{min} jumped to higher values. Therefore, under these conditions, it was no longer a good approximation to assume that all domains corresponded to the same value of dipolar moment/charge.

As already mentioned above, the calculated Debye–Hückel screening length (k^{-1}) was 0.55 nm for solutions with NaCl and almost 8 times higher (4.3 nm) for solutions without NaCl. Even for the closest interdomain separation observed, which was of the order of micrometers, the interdomain separation was higher than k^{-1}. For systems with NaCl, the interdomain separation was 3 orders of magnitude larger than k^{-1}, and in the systems without NaCl, it was 2 orders of magnitude larger. In other words, even without adding NaCl to the subphases, the domain charge may be screened and the interdomain interaction might be ruled by dipole–dipole repulsion according to Andelman et al.[19] Nevertheless, it appears that, even at conditions of low κ^{-1} (compared to the distances that characterized the texture of the monolayer), there was an effect of ionic strength on the interdomain interaction regimes (affecting the radial dependence of the interaction energies). It is important to remark here that we only compared our results with the expected behavior of domains following eq 1 or 2 and we did not scan all other possible regimes.

From the obtained Num values, the magnitudes of q and μ were calculated using eq 1 or 2, according to the better fitting model. These values were then normalized by the mean area of the domains (A), and thus, q/A and μ/A indicated the excess charge and dipole density, respectively, of the liquid-condensed phase in relation to the liquid-expanded one. In Figure 5C and D, q/A and μ/A are plotted together with their errors, derived from the error in the determination of Num and the size dispersion of the domains (see histograms in Figure 2A).

For dpPG in the absence of NaCl, the value of q/A was in the order of 10^{-8} elementary charges/Å^2 (Figure 5C). That is to say, the excess charge density in the condensed phase, compared to the expanded one, was 1 in 10^{-8} Å^2. Now, considering only the differences in molecular density (taking MMA equal to 100 and 60 Å^2 for liquid-expanded and liquid-condensed, respectively), an excess charge density of 10^{-2} elementary charges/Å^2 would be expected. Thus, if a radial dependence of r^{-1} was a consequence of a Coulomb interaction, this should correspond to a very low proportion (10^{-6}/Å^2) of nonscreened molecules. This is in keeping with the observation that interdomain separation was 2 orders of magnitude larger than k^{-1} for this system and with the fact that modeling of this system with eq 2 is also acceptable (RMS_{min} values in the range 10–15). For this system, μ values were also calculated (from the Num values obtained by comparing the experimental g_r with the simulated g_r obtained by the use of eq 2). The calculated μ/A were in the order of 10^1 mD/Å^2 for all the studied systems (Figure 5D). This is in agreement with the value estimated from $\Delta(\Delta V)$, considering that μ/MMA = $\Delta(\Delta V)/(6 \times \pi)$, where μ is expressed in mD, $\Delta(\Delta V)$ in mV, and MMA in Å^2 (adapted from Gaines[32] with $\varepsilon = 2$), leading to 9 mD/Å^2 using $\Delta(\Delta V)$ = 170 mV.

In summary, the domain distributions of dpPG monolayers at low %Ac and high I were good modeled considering point dipoles, similar to neutral domains. For the case of dpPG monolayers on low I subphases, it was not possible to ascertain an interaction model using the comparison of the experimental and simulated $g(r)$ under low %Ac conditions.

3.4. Diffusion of the Liquid-Condensed Domains. In order to get insight of the interdomain interactions in a broader range of %Ac values, the motion of domains was studied as an indirect way of evaluating domain–domain repulsions. The diffusion of domains was determined as explained in section 2.2.3, following the trajectory of two domains of comparable sizes, ranging from 1 to 3 μm radius. The diffusion coefficient of domains of these sizes inserted in an expanded phase (surface viscosity of the order of 10^{-10} N s m^{-1} [6,7]) depends only on the subphase viscosity (η_w) and their size according to[25]

$$D_t = k_B T/8\eta_w R \quad (4)$$

where k_B is the Boltzmann constant, T the temperature, η_w = 0.001 N s m^{-2} is the viscosity of water, and R is the radius of the pair of domains analyzed.

In the absence of interdomain interactions, the value of the diffusion coefficient determined experimentally (D_{exp}) should equal the value of the calculated diffusion coefficient (D_t, eq 4) for all the analyzed lateral pressures, since only a slight change in the intrinsic viscosity of the continuous phase (not enough to affect domain motion) would be expected in this small range of lateral pressures (from 6.5 to about 9 mN/m). For monolayers composed of sphingomyelin and ceramide, only a 2-fold change in the apparent viscosity was reported with a change of lateral pressure from 5 to 15 mN/m. Furthermore, this change was more related to an increase in the domain density than to a change in the intrinsic viscosity of the continuous phase.[7] Therefore, a departure in the values of D_{exp} compared to D_t was assigned to the presence of domain–domain interactions (hydrodynamic and electrostatic repulsions) that precluded the movement of the analyzed domains

dx.doi.org/10.1021/jp408053a | J. Phys. Chem. B 2014, 118, 519–529

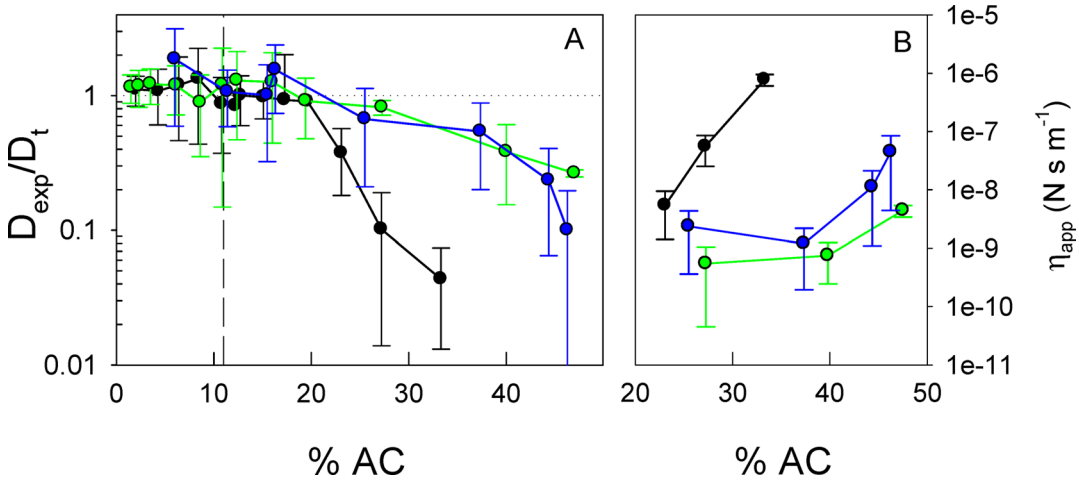

Figure 6. (A) Diffusion coefficients normalized by the diffusion coefficient for a monolayer with negligible viscosity and interdomain interactions. At the left of the vertical discontinuous line, the %AC variation was obtained by compression of the monolayer, whereas, at the right, higher %AC resulted from the application of an electric field. (B) Apparent surface viscosity as a function of %AC calculated from the diffusion coefficient of domains following the model of Hughes et al.[25] Symbols: dpPG monolayers in the presence (green) and absence (black) of NaCl in a Tris buffer subphase at 21 °C and neutral lipids on NaCl (blue) at 23 °C (data modified from ref 6).

and thus translated to a lower value of D_{exp} compared to the expected value according to the theory (D_t). Interdomain interactions should be more noticeable as the interdomain distances decrease, and thus, in Figure 6A, the relation D_{exp}/D_t was evaluated as a function of %Ac. In this plot, the data correspond to the average of the D_{exp}/D_t values obtained from the tracking of at least three pairs of domains in an environment of %Ac within the corresponding %Ac value ±3, and the error bars correspond to the standard deviation.

Monolayers with %Ac up to ∼10% (vertical dashed line in Figure 6A) were generated by compression, with a consequent rise in the lateral pressures of about 2.5 mN/m and an increase in the domain sizes and their polydispersity (see Figure 2). For these conditions, we selected the smallest domains (sizes in the range 1 μm < R < 3 μm) and followed their trajectories. As further compression would lead to an increase in the size of the domains with the probability of finding domains with R < 3 μm decreasing, to explore the region of %Ac higher than ∼10%, the surface pressure was maintained at 7−8 mN/m and an appropriate electric field was applied over the monolayer as explained in section 2.2.2. In this manner, domains could be recruited before the electric field was turned off and videos were recorded. This allowed exploration of a higher %Ac for the same domain size than at lower %Ac.

From Figure 6A, it can be observed that, for low values of % Ac (negligible domain−domain interactions), D_{exp}/D_t values of 1 were found. This indicates that the method for quantifying the diffusion coefficient yielded accurate values; i.e., neither convection drag nor any inaccuracy in the determination of the center of mass of the domains noticeably affected the Brownian motion determination. In addition, Figure 6A shows that D_{exp}/D_t equals 1 for regions of domains recruited by an electric field (right side of the vertical dashed line) up to about 20% of %Ac, indicating that the slow relaxation of this recruited area did not affect the determination of D_{exp}.

At %Ac values higher than 20%, a decrease of D_{exp}/D_t could be observed in a fashion that depended on the system studied. For dpPG monolayers in the absence of NaCl, D_{exp}/D_t dropped sharply to values lower than 1, reaching 0.1 at a value of %Ac of about 25%, whereas, in the presence of NaCl, this decrease started at higher %Ac and was in a less pronounced fashion, reaching D_{exp}/D_t = 0.3 at about 45%. In Figure 6A, the diffusion coefficients obtained for monolayers composed of dsPC and dmPC on 0.15 M NaCl are also plotted for comparison. These D_{exp}/D_t values were calculated from experimental results previously reported by our group,[6] which were then divided by the theoretically expected value (D_t) according to each domain size (data previously obtained). It can be observed that dpPG monolayers on subphases containing Tris and NaCl at 21 °C exhibited the same trend as neutral lipid monolayers on NaCl solutions at 23 °C, with the latter reaching D_{exp}/D_t = 0.1 at %Ac > 45%. At 30%Ac, both charged monolayers on high ionic strength and neutral monolayers significantly differ from charged monolayers on a low ionic strength subphase. In other words, at a different range of %Ac values than that analyzed in sections 3.2 and 3.3 and using a dynamic property, charged lipid monolayers also exhibited a different behavior at low and high ionic strengths with the latter behaving similar to neutral monolayers.

Hughes et al.[25] described the dependence of the diffusion coefficient of a cylinder inserted in a continuous membrane with surface viscosity η. In the systems showed here, the observed decrease in the diffusion coefficients is not related to a change in the intrinsic viscosity of the expanded phase but to interdomain interactions that preclude domain motion. However, the domain environment may be considered as a continuous medium with an apparent surface viscosity η_{app} (mean filed approximation), and from the D_{exp} values, η_{app} can be estimated. The calculation was performed as explained in refs 6 and 7 for conditions of high %Ac, since, as already stated, at low %Ac values, D_t follows eq 4. The obtained η_{app} values are plotted in Figure 6B where it is shown that the apparent viscosity increased with %Ac and that, for monolayers of dpPG on subphases of low I, η_{app} reached the highest values at lower %Ac.

In summary, at low %Ac values, interdomain interaction did not appreciably affect the diffusion coefficient of the domains, while, at high %Ac, domain motion was precluded. Under these conditions, different behavior was observed for the charged domains at different ionic salt concentrations, which derived in

dx.doi.org/10.1021/jp408053a | J. Phys. Chem. B 2014, 118, 519−529

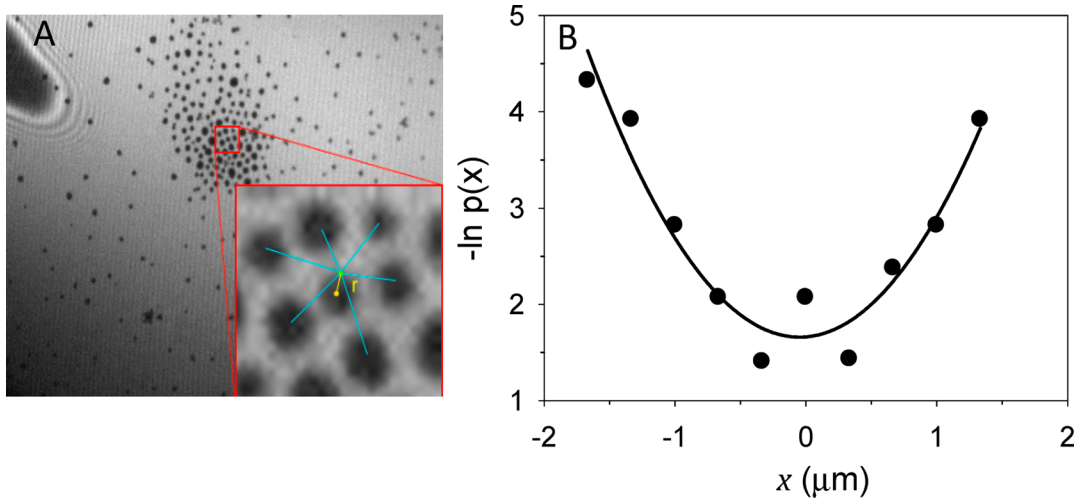

Figure 7. (A) Example of an array of domains at high %Ac. The position of the domain with respect to the center of mass of the array was determined for the calculation of k. (B) Logarithm of the histograms of x (symbols) and fitting of the data with eq 5 (line).

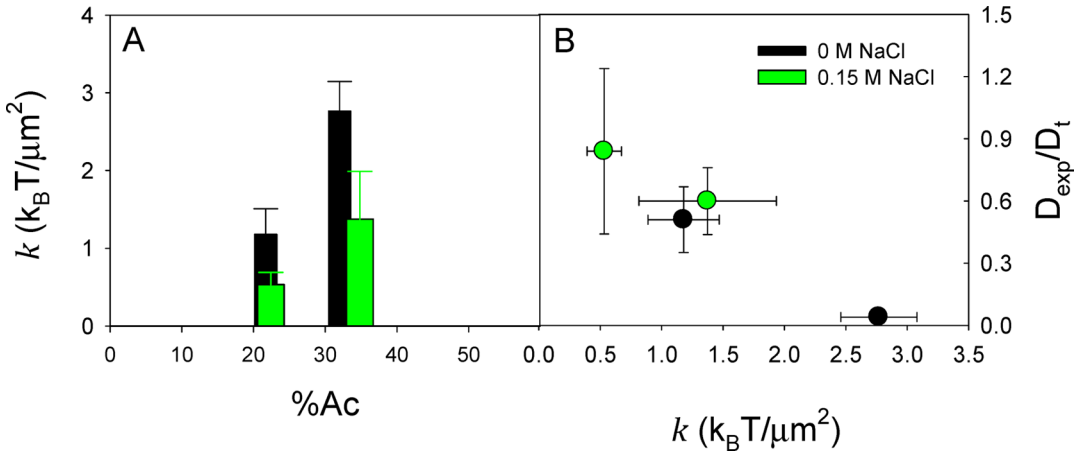

Figure 8. (A) Spring constant (k) determined at high %Ac values for both ionic strengths. (B) Correlation between k and the normalized diffusion coefficient (D_{exp}/D_t).

a higher apparent surface viscosity for monolayers on subphases with low I at comparable %Ac values.

3.5. Quantification of Interactions between Domains at High %Ac Regimes. Figure 6 shows that, for a percentage of condensed area in the range from 20 to 40%, the diffusion of charged domains was modified by the concentration of ions in the subphase, and when the NaCl concentration was high, charged domains followed the same trend as neutral domains. This difference may have been related to higher domain−domain repulsions for charged domains in the absence of NaCl, which could have been hydrodynamic or electrostatic interactions. However, the hydrodynamic interactions did not seem to be involved, since the neutral domains followed the same trend as the dpPG domains with NaCl in the subphase, whereas the salt changed the behavior in monolayers composed of the same lipid.

As already mentioned above, at high %Ac values, the approach employed in section 3.3 is not straightforward, since the size and shape of the domains, as well as the polydispersity, should be considered in the simulated experiments because point dipole and point charge are no longer good approximations. Therefore, in order to gain better insight into the interdomain interactions in this region of %Ac, the distributions of positions of a central domain relative to the center of mass of an array of domains were determined as follows.[11,33] First, consider a central domain surrounded by its six nearest neighbors, whose combined imposed potential is given by U. Then, for an equilibrium situation, the probability p of finding the central domain at a distance r from the center of mass of the neighbors is proportional to the Boltzmann factor, i.e., $p = C \exp(U/k_BT)$. An example of the determination of r is shown in Figure 7A, and as this is a distribution of positions and not a dynamic measurement, then the hydrodynamic interactions should not influence the results and only the electrostatic repulsion will be obtained by this approach. It is worth pointing out that, in these experiments, since the analyzed region was a zone where the domain density was locally increased with an electric field, the distribution of the domain positions in the whole monolayer was not homogeneous and, thus, it was not in a global equilibrium. However, it is expected that a central domain in a hexagonal array (surrounded by at least two rings of domains) moves in the potential trap generated by the other domains, showing a distribution of positions that depends on this local potential minimum. Therefore, a Boltzmann distribution was used, assuming local equilibrium.

dx.doi.org/10.1021/jp408053a | J. Phys. Chem. B 2014, 118, 519−529

As previously explained, the high %Ac values were obtained by applying an attractive electric field on monolayers presenting small domains with a sharp distribution of sizes (8 and 7 mN/m for systems with NaCl and without NaCl, respectively, see Figure 2A). In this way, it was possible to observe domain arrangements where a central domain was surrounded by 5−8 closest neighbors. For the determination of the distribution of the positions, the center of mass of selected six-neighbor arrangements (see Figure 7A as an example) was calculated and the position $\vec{r} = (x, y)$ of the central domain with respect to the center of mass was determined for each frame of 15 s videos (150 frames).

Histograms for x and y values were computed (see symbols in Figure 7B) and no significant differences were found, which led us to consider a radially symmetric probability distribution. The loss of the angular dependence arised as a consequence of averaging the positions of the six surrounding domains over the considered time period.

For conditions of crowded domains, we assumed that both in the presence and in the absence of NaCl the interaction potentials had the same dependence on x (or y, since there is radial symmetry) in the form of a harmonic potential, i.e., $U_{(x)} = (1/2)kx^2$. This implies for $p(x)$

$$-\ln(p(x)) = \frac{kx^2}{2k_BT} - \frac{C}{k_BT} \quad (5)$$

Figure 7B shows an example where the logarithm of the distribution was fitted with eq 5. These fittings yielded R values between 0.88 and 0.98. In Figure 8A, the spring constants k obtained through this method are plotted for dpPG monolayers in the absence and in the presence of NaCl at %Ac where the diffusion coefficient suggested different interdomain interactions. For %Ac around 20%, the dpPG monolayers presented higher interaction potentials (higher k values) in the absence of NaCl. At higher %Ac (>30%), the k values in the presence of NaCl had similar values to those at lower %Ac in the absence of NaCl. These values were compared with those obtained from diffusion measurements. As the %Ac between both techniques didn't match exactly, the D_{exp}/D_t values were interpolated following the lines in Figure 6A, in order to obtain the same % Ac as those used for the spring constants. Interestingly, there was a clear correlation of k with the diffusion coefficients; Figure 8B shows that D_{exp}/D_t increased concomitantly with a decrease in k, with this behavior appearing to be independent of the subphase ionic strength. In other words, the ionic strength modulated the electrostatic repulsions (the k value), and in turn, k regulated the diffusion of the domains. At ∼30% of the condensed area, the domains in the absence of NaCl presented considerably higher k values, thus explaining the abrupt drop in the diffusion coefficient.

4. CONCLUSIONS

In this study, interdomain interactions for micrometer-sized domains formed by charged surfactants were analyzed and compared with domains formed by neutral lipids. These interactions were investigated at different interdomain distances and on subphases of different ionic strength; at low %Ac and at high %Ac, different approaches were used and the effect of these interactions on the monolayer rheology was studied in a broad range of %Ac. For low percentages of condensed area (high interdomain distances), the domains were considered to be point charges or dipoles and the interaction regime was determined, i.e., the Coulomb and dipolar interaction models were evaluated. Experimental results for charged domains at high ionic strength were fitted better by the dipolar model, whereas, at low ionic strength, although the Coulomb model yielded a better fit, dipolar interactions also modeled the system acceptably. Furthermore, both the excess surface charge and the excess dipole density that were obtained from the fitting process were physically possible and, thus, the interaction regime in this system could not be ascertained. At these low conditions of %Ac, interdomain interactions did not affect the monolayer rheological properties in all the analyzed conditions.

At lower interdomain distances, a more marked differential behavior between the studied systems was observed: on subphases of high ionic strength, charged domains interacted in a similar manner to neutral domains. The interdomain interaction highly precluded domain motion at about 45% of condensed area, as previously reported for neutral domains,[6,7] while, on low ionic strength subphases, domain motion was precluded at lower %Ac. A good correlation was found between domain−domain repulsion and the decrease in the domain diffusion coefficient.

At the lower ionic strength condition that was analyzed in this study, the Debye−Hückel length was still 2 orders of magnitude lower than the interdomain distances, but the interdomain interactions nevertheless were able to reflect the decrease in the charge screening, with a stronger repulsion potential being observed. This increase in the interdomain repulsion translated to a lower domain motion, and consequently a higher apparent viscosity at a similar percentage of condensed areas when compared to systems with higher salt concentrations.

In summary, our results show that, for charged two-phase monolayers, the ion concentration regulates interdomain interactions still at conditions where the interdomain distances are 2 orders of magnitude higher than the Debye−Hückel distance and that, in turn, domain−domain electrostatic interactions are able to regulate the film rheological properties.

■ ASSOCIATED CONTENT

Supporting Information

S1: Compression isotherms for dmPC and dsPC on Tris or Tris + NaCl subphases. S2: Procedure to convert an image from a scale of gray to a binary image. S3: Automatic domain tracking on monolayer videos. S4: Ionization degree of dpPG as a function of bulk pH. S5: Error in the determination of the parameter Num, which led to a minimal RMS (RMS_{min}) between the experimental and simulated $g(r)$ curves. S6: Radial distribution functions obtained experimentally and from molecular dynamics simulations $g(r)$ for the four systems analyzed at different %Ac. Movie: Representative experiment showing that the relaxation of the region recruited of domains was slow and it could be neglected. Real size: 343 μm × 262 μm. Real time: 20 s. Conditions: dpPG monolayer on 5 mM Tris and 0.15 M NaCl. This material is available free of charge via the Internet at http://pubs.acs.org.

■ AUTHOR INFORMATION

Corresponding Author

*E-mail: wilke@mail.fcq.unc.edu.ar. Phone/fax: +54-351-4334171.

Notes

The authors declare no competing financial interest.

■ ACKNOWLEDGMENTS

This work was supported by SECyT-UNC, CONICET, and FONCYT (Program BID 0770), Argentina. N.W., M.V., and L.R. are career investigators and B.C. is a posdoctoral fellow of CONICET.

■ REFERENCES

(1) Cicuta, P.; Keller, S. L.; Veatch, S. L. *J. Phys. Chem. B* **2007**, *111*, 3328.
(2) Ding, J.; Warriner, H. E.; Zasadzinski, J. A. *Phys. Rev. Lett.* **2002**, *88*, 168102.
(3) Saxton, M. J. *Biophys. J.* **1993**, *64*, 1053.
(4) Selle, C.; Ruckerl, F.; Martin, D. S.; Forstner, M. B.; Kas, J. A. *Phys. Chem. Chem. Phys.* **2004**, *6*, 5535.
(5) Forstner, M. B.; Martin, D. S.; Ruckerl, F.; Kas, J. A.; Selle, C. *Phys. Rev. E: Stat., Nonlinear, Soft Matter Phys.* **2008**, *77*, 051906.
(6) Wilke, N.; Vega Mercado, F.; Maggio, B. *Langmuir* **2010**, *26*, 11050.
(7) Wilke, N.; Maggio, B. *J. Phys. Chem. B* **2009**, *113*, 12844.
(8) Bhalla, U. S.; Iyengar, R. *Science* **1999**, *283*, 381.
(9) Vereb, G.; Szollosi, J.; Matko, J.; Nagy, P.; Farkas, T.; Vagh, L.; Matyus, L.; Waldmann, T. A.; Damjanovich, S. *Proc. Natl. Acad. Sci. U.S.A.* **2003**, *100*, 8053.
(10) Nassoy, P.; Birch, W. R.; Andelman, D.; Rondelez, F. *Phys. Rev. Lett.* **1996**, *76*, 455.
(11) Semrau, S.; Idema, T.; Schmidt, T.; Storm, C. *Biophys. J.* **2009**, *96*, 4906.
(12) Rückerl, F.; Käs, J. A.; Selle, C. *Langmuir* **2008**, *24*, 3365.
(13) McConnell, H. M. *Annu. Rev. Phys. Chem.* **1991**, *42*, 171.
(14) Wurlitzer, S.; Fischer, T. M.; Schmiedel, H. *J. Chem. Phys.* **2002**, *116*, 10877.
(15) Hartmann, W.; Galla, H. J.; Sackmann, E. *FEBS Lett.* **1977**, *78*, 169.
(16) Vequi-Suplicy, C. C.; Riske, K. A.; Knorr, R. L.; Dimova, R. *Biochim. Biophys. Acta* **2010**, *1798*, 1338.
(17) Shimokawa, N.; Hishida, M.; Seto, H.; Yoshikawa, K. *Chem. Phys. Lett.* **2010**, *496*, 59.
(18) Cëbers, A.; Janmey, P. A. *J. Phys. Chem. B* **2002**, *106*, 12351.
(19) Andelman, D.; Brochard, F.; Joanny, J.-F. *J. Chem. Phys.* **1987**, *86*, 3673.
(20) Wilke, N.; Dassie, S. A.; Leiva, E. P.; Maggio, B. *Langmuir* **2006**, *22*, 9664.
(21) Miller, A.; Möhwald, H. *Europhys. Lett.* **1986**, *2*, 67.
(22) Wilke, N.; Maggio, B. *Biophys. Chem.* **2006**, *122*, 36.
(23) Miller, A.; Helm, C. A.; Möhwald, H. *J. Phys. (Paris)* **1987**, *48*, 693.
(24) Sbalzarini, I. F.; Koumoutsakos, P. *J. Struct. Biol.* **2005**, *151*, 182.
(25) Hughes, B. D.; Pailthorpe, B. A.; White, L. R. *J. Fluid Mech.* **1981**, *110*, 349.
(26) Egorova, E. M. *Colloids Surf., A* **1998**, *131*, 7.
(27) Vega Mercado, F.; Maggio, B.; Wilke, N. *Chem. Phys. Lipids* **2011**, *164*, 386.
(28) Grigoriev, D.; Krustev, R.; Miller, R.; Pison, U. *J. Phys. Chem. B* **1999**, *103*, 1013.
(29) Ruckenstein, E.; Li, B. *J. Phys. Chem. B* **1998**, *102*, 981.
(30) Aroti, A.; Leontidis, E.; Maltseva, E.; Brezesinski, G. *J. Phys. Chem. B* **2004**, *108*, 15238.
(31) Wurlitzer, S.; Schmiedel, H.; Fischer, T. M. *Langmuir* **2002**, *18*, 4393.
(32) Gaines, G. L., Jr. *Insoluble monolayers at liquid-gas interfaces*; John Wiley & Sons, Inc: New York, 1966.
(33) Rozovsky, S.; Kaizuka, Y.; Groves, J. T. *J. Am. Chem. Soc.* **2005**, *127*, 36.